DYNAMIC RESPONSE AND SOUND RADIATION OF TEXTILE-REINFORCED COMPOSITE SHELLS

Hufenbach, W.*, Täger, O.*, Dannemann, M.*

[Hufenbach, W.] ot@ilk.mw.tu-dresden.de

* Technische Universität Dresden,

Institute of Lightweight Structures and Polymer Technology (ILK), D-01062 Dresden

Keywords: *Textile shells, anisotropic damping, structural-dynamics, acoustic design, coupled FE/BE analysis*

Abstract

Lightweight structures for high-technology applications increasingly have to fulfill not only high demands on stiffness and strength but also on high damping and low sound radiation due to the rising comfort requirements. Here, textile-reinforced composites offer a very high vibro-acoustic lightweight potential. The great number of textile-specific design variables allows to synergetically fulfill high stiffness and acoustic standards.

This paper makes a contribution to the development of such low noise textile-reinforced lightweight composite structures by analyzing the structural-dynamic response and sound radiation of textile-reinforced composite shells. Based on a textile-adapted determination of secured dynamic elasticity and damping values as well as acoustic properties of different textile-reinforced composites the authors developed numerical vibro-acoustic simulation models. These models allow to calculate the complicated deformation and sound radiation behavior of textile-reinforced composite shells. Detailed parameter studies show the complex coupling of material anisotropy and geometry, which influences both the structural-dynamic and sound radiation characteristics of composite shells.

1 Introduction

Lightweight structures made of textile-reinforced composite materials are increasingly used in many fields of high-technology applications due to their versatile property profile [1]. Especially for sophisticated aerospace and spacecraft applications, low constructive weight and adequate stiffness combined with high material damping as well as a low sound radiation are required. Here, anisotropic textile composites offer a high lightweight acoustic potential. The specific combination of different materials and the large variety of textile architectures give the possibility of synergetically fulfilling the pretentious demands on stiffness, damping and acoustic behavior.

As practically relevant demonstrators this paper focuses on the vibro-acoustic behavior of textile-reinforced composite shells (TCS). The vibro-acoustic design of such multilayered TCS is complicated due to the anisotropic textile material and the complex deformation behavior. This challenging task is solved within this paper by a combined numerical and experimental analysis. The determination of the visco-elastic dynamic and acoustic material properties of different textiles was done using resonance bending tests and sound intensity measurements within an Acoustic Window Test Stand (AWS), respectively. On this basis, the structural-dynamic, damping and sound radiation behavior of TCS was analyzed by coupled Finite and Boundary Element calculations using the concept of complex moduli for visco-elastic materials.

2 Visco-elastic material parameters of textile-reinforced composites

The determination of the dynamic stiffness and material damping values is done for representative homogenized textile-reinforced single layers using material-adapted experiments. The authors used a special resonance bending system (according to DIN EN ISO 6721 [2], see Fig. 1) modified for composite materials in combination with the Fast-Fourier-Transformation (FFT).
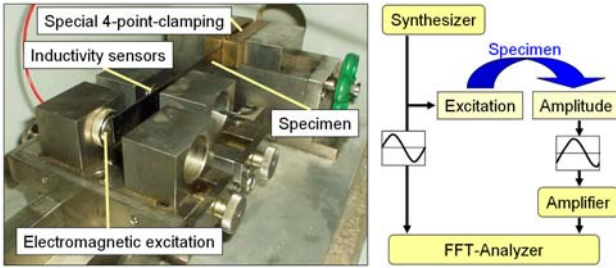
Fig. 1: Setup of the resonance bending test stand

The dynamic properties are measured using beam specimens with rectangular shape excited harmonically on the wider surface (see Fig. 1). The examinations of the directional-dependent dynamic material properties include tests on 0°, 30°, 45°, 60° and 90° reinforced specimens, where 0° corresponds to the direction of textile production (weft direction). Testing of 0° and 90° specimens enables to determine the dynamic YOUNG's modulus parallel and perpendicular to the production direction from the measured resonance frequencies (see HOLSTE [4]). The shear modulus is calculated using the following polar transformation

$$\frac{1}{E'_x(\varphi)} = \frac{1}{E'_\parallel}\cos^4\varphi + \frac{1}{E'_\perp}\sin^4\varphi + \left(\frac{1}{G'_\#} - 2\frac{\nu_{\parallel\perp}}{E'_\parallel}\right)\sin^2\varphi\cos^2\varphi. \quad (1)$$

Thus, the shear modulus $G'_\#$ is calculated using the Young's modulus E'_{45} of the 45° specimen

$$G'_\# = \frac{E'_{45}}{4 - \left(1 - 2\nu_{\parallel\perp}\right)\dfrac{E'_{45}}{E'_\parallel} - \dfrac{E'_{45}}{E'_\perp}}. \quad (2)$$

The damping values $d_\parallel$, $d_\perp$ and $d_\#$ of the textile composite single layers are also determined using the resonance bending test. According to DIN EN ISO 6721 [2] the damping can be derived from the 3dB-bandwidth of the resonance curve. Testing of 0° and 90° specimens, respectively, yields to the damping values $d_\parallel$ and $d_\perp$. Analogue to the determination of the shear modulus, the shear damping $d_\#$ is calculated by polar transformation (see HOFFMANN [6] and ADAMS [7]). Thus, the shear damping $d_\#$ can be calculated using the damping value d_{45} of the 45° specimen

$$d_\# = G'_\#\left[\frac{4d_{45}}{E'_{45}} - \left(1 + \nu_{\parallel\perp}\left(1 + \frac{d_\perp}{d_\parallel}\right)\right)\frac{d_\parallel}{E'_\parallel} - \frac{d_\perp}{E'_\perp}\right]. \quad (3)$$

The specimens are fixed on one side in a special 4-point-clamping developed to minimize the energy loss within the clamping zone while the other end remains free. Small thin iron washers are attached on the surface of the specimen allowing electromagnetic excitation. The amplitude of the forced flexural vibration is registered contactless with inductivity sensors. The resonance frequency and the corresponding 3dB-bandwidth can be determined from the resulting resonance curve, which is calculated by FFT.

For a fast and secure testing of the statistically necessary big amount of specimens, an adapted software tool with a graphical user interface "RESOPRUEF" was written at the ILK (Fig. 2).
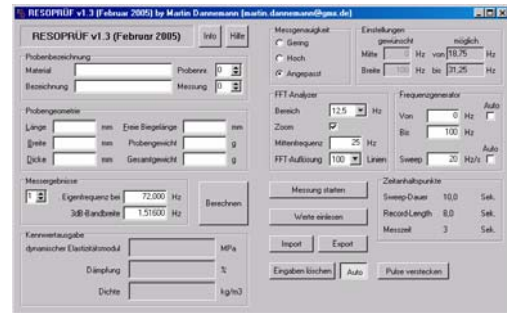

Fig. 2: Graphical user interface RESOPRUEF

This tool enables the user to access all important parameters for determining the dynamic properties in one step. The software itself is linked to commercial FFT software, which is responsible for doing the measurements.

Using this measurement procedure the dynamic stiffness parameters and damping values of composites with different types of reinforcing fibers (carbon and glass) and different textile architectures (e.g. woven and knitted fabrics) were determined. Fig. 3 shows a comparison of the dynamic YOUNG's modulus and the material damping for carbon and glass epoxy based composites with twill woven reinforcement.

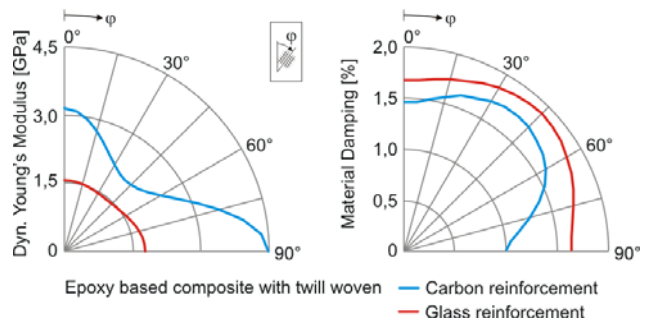Epoxy based composite with twill woven — Carbon reinforcement — Glass reinforcement

Fig. 3: Polar diagrams of dynamic YOUNG's modulus and material damping for epoxy based composites reinforced with twill woven carbon and glass fabrics

The directional dependence of the dynamic Young's modulus of the carbon fiber reinforced composite shows an almost bidirectional characteristic with maximum values at 0° and 90°. Whereas, the anisotropy of glass fiber composite is much smaller. The absolute values significantly differ for the different fibers. As expected, the composite with the carbon fibers shows the highest stiffness compared to the glass fiber reinforcement. The material damping shows an opposite behavior. Here, the highest damping values were measured for the glass reinforcement.

The characteristics of the dynamic material properties for GF/EP based composites reinforced with woven and three different knitted fabrics are shown in Fig. 4. The knitted fabrics differ in yarn size, fabric thickness and yarn quantity. Knitted fabric #1 and #2 contain 1 or 2 1200tex yarns in weft direction and 1 or 2 900tex rovings in warp direction, respectively. The knitted fabric #3 is set up from 600tex yarns in weft direction and 900tex yarns in warp direction. Furthermore, the thickness of the specimen with knitted reinforcement #2 is approx. twice as much as these with #1 or #3.
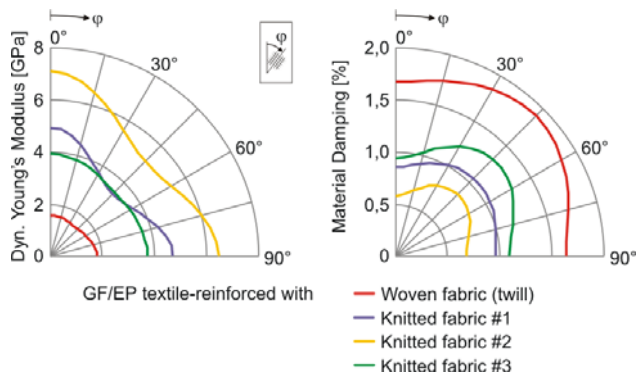

Fig. 4: Characteristics of dynamic Young's modulus and material damping for different epoxy based glass fiber reinforced composites

The knitted composites #1 and #3 show different stiffness characteristics but nearly comparable stiffness values. Whereas, the knitted composite #2 has the highest stiffness due to its higher thickness. The composite with woven fabric shows much smaller stiffness values than the composites with knitted reinforcements due the high yarn ondulation of the woven fabric. For the material damping an opposite behavior is found. Here, the highest damping values for the composites with woven reinforcements were measured, because of the higher influence of the viscoelastic matrix material and the higher friction between the fibers.

3 Experimental determination of acoustic properties of composites

The acoustic investigations were carried out within an AWS consisting of a reverberant and a sound absorbing chamber [3]. The sound waves inside the reverberant chamber are reflected on all of the rigid walls, so that a diffuse sound field is created. This diffuse sound field is then taken as the acoustic excitation of a test structure, which is clamped inside a test window between the reverberant and sound absorbing chamber. The transmitted sound power is analyzed inside the absorbing chamber using a sound intensity probe (see Fig. 5).
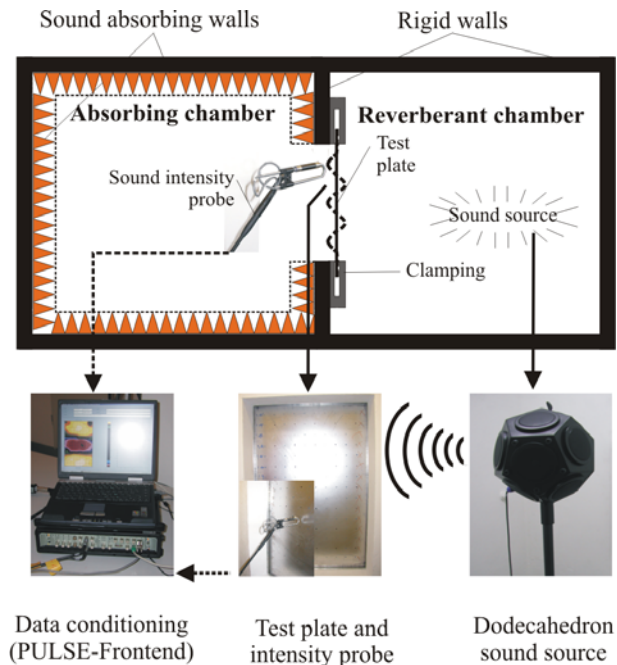

Fig. 5: Experimental setup within the AWS

In order to determine the acoustic property profiles of different textiles, the radiated sound power of CF/PEEK, CF/EP and GF/EP composites was measured and the influence of their fiber and matrix systems on the sound radiation was identified (see Fig. 6).
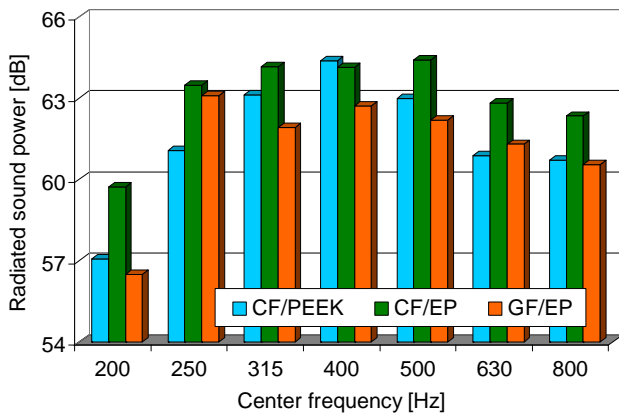
Fig. 6: Radiated sound power levels of different textile-reinforced composite materials

A comparison of the sound power levels of the different CF-reinforced composites reveals the acoustic influence of the matrix material. In most of the 3rd octave bands, the CF/PEEK compound radiates less sound power than the CF/EP compound. Especially, for the lower frequencies up to 2 dB lower sound power levels have been measured. Furthermore, the GF/EP composite radiates less sound power over the whole frequency range compared to the CF/EP composite. Thus, for high damping applications a composite reinforced with glass fibers should be preferred.

4 Numerical vibro-acoustic analyses of textile-reinforced composite shells

The structural-dynamic behavior of TCS is rather complex due to the coupled effects of shell geometry and material anisotropy. The resulting complicated states of deformation determine the excited surface velocity fields and therefore the sound radiation. Thus, the vibro-acoustic properties of TCS are influenced by both material anisotropy and geometric parameters. In order to investigate this complex structural-dynamic and sound radiation behavior the authors developed material- and geometry-adapted numerical vibro-acoustic models for TCS.

4.1 Description of the numerical vibro-acoustic models

The structural-dynamic analysis of the TCS was performed using a Finite Element (FE) code allowing to include the anisotropic material behavior within the modal and response analysis. The effects of material damping were modeled using the concept of complex visco-elastic moduli [4]. For the calculation of the sound radiation the structural-dynamic FE models were coupled with

corresponding Boundary Element (BE) models in order to project the structural modes on the fluid surface of the TCS. Fig. 7 shows the used fluid surfaces of the acoustic BE models and the defined acoustic properties.
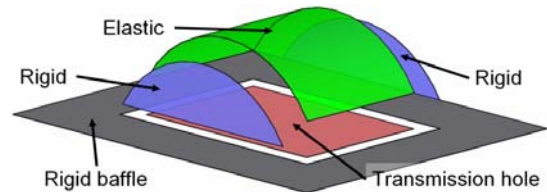

Fig. 7: Fluid surfaces and acoustic properties within the used BE models

The BE models were build as a transmission set-up consisting of a transmitter and a receiver hall separated by a rigid baffle (see Fig. 8).
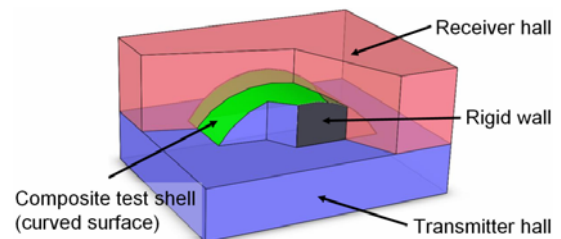

Fig. 8: Acoustic BE model set-up

A diffuse sound field within the transmitter hall was taken as excitation of the TCS. The resulting surface velocity fields of the TCS have been calculated on the basis of the results of the modal analysis. The implementation of adequate vibro-acoustic coupling conditions within the BE models then allows to calculate the sound power radiation of the acoustically excited TCS into the receiver hall.

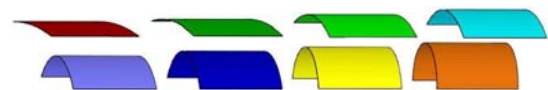Fig. 9 shows the investigated TCS geometries.

Fig. 9: Investigated TCS geometries

All TCS have the same width of 560 mm, a length of 860 mm and a thickness of 2 mm. Thus, the surface area of the investigated composite shells stays constant. The shell curvature is varied from 0,25 to 3,65 m^{-1} in 7 steps.

4.2 Results

The developed coupled FE/BE models for TCS were used to perform extensive parameter studies [5] in order to identify the influence of shell curvature and fiber orientation on sound radiation. Fig. 10 exemplarily shows the radiated sound power of the

investigated TCS in dependence of the shell curvature. Here, for each curvature the sound radiation of the 2/1 mode[1] was calculated.
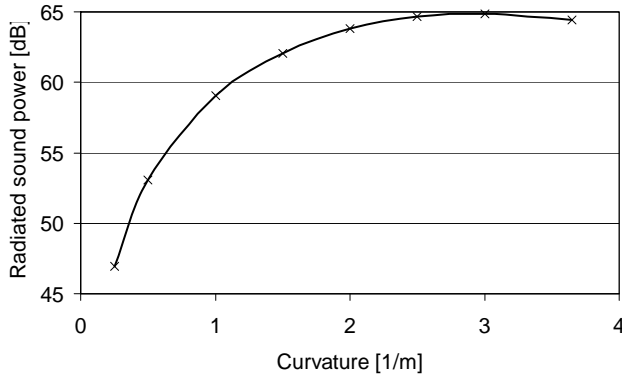

Fig. 10: Calculated sound power level in dependence of shell curvature (2/1 mode)

The calculations clearly reveal, that an increasing curvature causes higher sound power levels for the 2/1 mode shape. Furthermore, a saturation of sound radiation increase was found at a curvature of 3 m^{-1}. This behavior can be explained by the change of the TCS stiffness with increasing shell curvature. Fig. 11 shows the calculated sound power in dependence of the frequency of the 2/1 mode for the investigated curvatures.
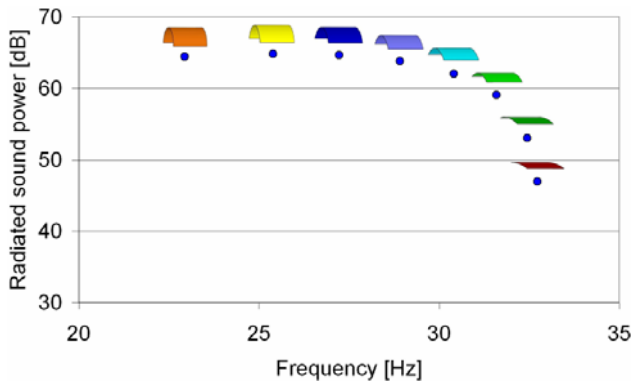

Fig. 11: Radiated TCS sound power of 2/1 mode over frequency

Here, it can be seen, that the frequency of the 2/1 mode decreases for the TCS with high curvatures. Thus, the corresponding shell stiffness is smaller for higher curvatures resulting in higher vibration amplitudes of the TCS. Consequently, the TCS with higher curvatures radiate more sound power.

The influence of different fiber orientations on the radiated sound power level of the 2/1 mode is

---

[1] The shell modes are numbered by n/m, where n counts the deflection maxima parallel to the curved edge and m the maxima parallel to plane edge.

displayed in Fig. 12 in dependence of the investigated curvatures.
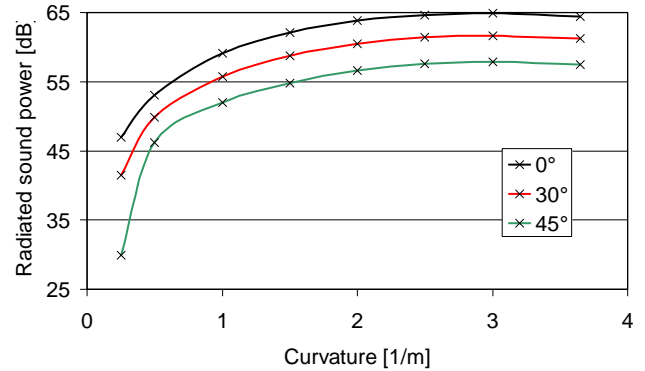

Fig. 12: Radiated TCS sound power for different fiber-orientations and curvatures

For all of the investigated fiber orientations the radiated sound power rises with increasing shell curvature due to the smaller TCS stiffnesses. Furthermore, a clear decrease of the sound power radiation for higher fiber angles has been found. Here, the drastically rising modal damping for high fiber angles creates a damping dominated sound radiation decrease.

5 Conclusions

The performed extensive experimental and numerical investigations clearly reveal the high vibro-acoustic lightweight potential of textile-reinforced composite shells. The high number of material and geometrical design variables give the possibility to synergetically fulfill the pressing demands on light structures with low sound radiation. But the complex coupling of material anisotropy and geometry creates complicated deformation and sound radiation characteristics of TCS. Thus, a successful vibro-acoustic design of TCS is only possible, if geometry- and material-adapted simulation tools are available, which account for the large variety of textile-reinforced composites and shell geometries. Here, the authors developed practice-oriented FE/BE models, which allow to perform parameter studies on the influence of textile- and shell-specific design variables on the sound radiation. These models are a valuable help for the design engineer and are a contribution for the development of light and low noise textile-reinforced composite shell structures.

References

[1] Haldenwanger, H.-G.: Komplexität des Leichtbaus in der Fahrzeugtechnik. *Dresdner Leichtbausymposium 2001*, Dresden, 2001

[2] DIN EN ISO 6721: *Plastics, Determination of dynamic mechanical properties*, Dezember 1996

[3] Täger, O.: *Beitrag zur Analyse der Strukturdynamik und Schallabstrahlung hybrider anisotroper Mehrschichtverbunde.* Dissertation, Technische Universität Dresden, 2003

[4] Holste, C.: *Zum Dämpfungsverhalten anisotroper Faserverbundstrukturen.* Dissertation, Technische Universität Clausthal, 1998

[5] Hufenbach, W.; Täger, O., Dannemann, M.: Numerical Design of Hybrid Carbon Composites for High Comfort Applications. *Proceedings of the 36th International SAMPE Conference*, San Diego, 15-18 November 2004

[6] Hoffmann, U.: *Zur Optimierung der Werkstoffdämpfung anisotroper polymerer Hochleistungs-Faserverbundstrukturen.* Dissertation, Technische Universität Clausthal 1992

[7] Adams, R. D.; Bacon, D. G. C.: Effect of Fibre Orientation and Laminate Geometry on the Dynamic Properties of CFRP, in: *Journal of Composite Materials*, Vol. 7, 1973, S. 402 428